Journal of the American College of Cardiology
© 2001 by the American College of Cardiology
Published by Elsevier Science Inc.

Vol. 38, No. 1, 2001
ISSN 0735-1097/01/$20.00
PII S0735-1097(01)01314-6

Myocardial Viability Assessment by Endocardial Electroanatomic Mapping: Comparison With Metabolic Imaging and Functional Recovery After Coronary Revascularization

Karl-Christian Koch, MD,* Juergen vom Dahl, MD, FESC,* Monika Wenderdel,* Bernd Nowak, MD,† Wolfgang M. Schaefer, PHD,† Alexander Sasse, MD,* Christoph Stellbrink, MD,* Udalrich Buell, MD,† Peter Hanrath, MD, FACC, FESC*

Aachen, Germany

OBJECTIVES The objective of this study was to compare electroanatomic mapping for the assessment of myocardial viability with nuclear metabolic imaging using positron emission computed tomography (PET) and with data on functional recovery after successful myocardial revascularization.

BACKGROUND Animal experiments and first clinical studies suggested that electroanatomic endocardial mapping identifies the presence and absence of myocardial viability.

METHODS Forty-six patients with prior (≥2 weeks) myocardial infarction underwent fluorine-18 fluorodeoxyglucose (FDG) PET and Tc-99m sestamibi single-photon emission computed tomography (SPECT) before mapping and percutaneous coronary revascularization. The left ventricular endocardium was mapped and divided into 12 regions, which were assigned to corresponding nuclear regions. Functional recovery using the centerline method was assessed in 25 patients with a follow-up angiography.

RESULTS Regional unipolar electrogram amplitude was 11.0 mV ± 3.6 mV in regions with normal perfusion, 9.0 mV ± 2.8 mV in regions with reduced perfusion and preserved FDG-uptake and 6.5 mV ± 2.6 mV in scar regions ($p < 0.001$ for all comparisons). At a threshold amplitude of 7.5 mV, the sensitivity and specificity for detecting viable (by PET/SPECT) myocardium were 77% and 75%, respectively. In infarct areas with electrogram amplitudes >7.5 mV, improvement of regional wall motion (RWM) from −2.4 SD/chord ± 1.0 SD/chord to −1.5 SD/chord ± 1.1 SD/chord ($p < 0.01$) was observed, whereas, in infarct areas with amplitudes <7.5 mV, RWM remained unchanged at follow-up (−2.3 SD/chord ± 0.7 SD/chord to −2.4 SD/chord ± 0.7 SD/chord).

CONCLUSIONS These data suggest that the regional unipolar electrogram amplitude is a marker for myocardial viability and that electroanatomic mapping can be used for viability assessment in the catheterization laboratory. (J Am Coll Cardiol 2001;38:91–8) © 2001 by the American College of Cardiology

Recently, a catheter-based nonfluoroscopic endocardial electroanatomic mapping system has been developed and validated in animal experiments (1,2). Since myocardial ischemia and infarction result in significantly reduced electrical parameters of the affected myocardium (3,4), the local endocardial electrogram has been proposed as an indicator of myocardial viability. The system's ability to provide information about regional electrical and mechanical properties of the left ventricle (LV) has previously been evaluated in animal models and in human studies (2,5–10).

The purpose of this study was to compare the assessment of myocardial viability in patients who have had a prior myocardial infarction (MI), and corresponding regional wall motion (RWM) abnormalities, by using the endocardial mapping system with the results obtained by using metabolic positron emission computed tomography (PET) imaging and with data on functional recovery after successful revascularization.

METHODS

Patients. Patients with previous MI (>2 weeks) and RWM abnormalities at rest and with a clinical indication for a percutaneous revascularization were included in this study. After diagnostic angiography and before balloon angioplasty or percutaneous recanalization, all patients underwent PET and single photon emission computed tomography (SPECT) imaging. In patients without evidence for maintained viability from the results of both PET/SPECT imaging and electroanatomic mapping, a percutaneous transluminal coronary angioplasty (PTCA) was performed when the procedure was thought to impose minimal risk on the patient and the target lesion was located in a large and dominant vessel. Echocardiography was performed one day before the intervention to exclude intraventricular thrombus. An additional biplane LV angiography was performed in all patients immediately before mapping

From the *Medizinische Klinik I (Department of Cardiology) and †Department of Nuclear Medicine, University Hospital, Aachen, Germany.

Manuscript received October 23, 2000; revised manuscript received March 7, 2001, accepted March 26, 2001.

Abbreviations and Acronyms

AUC	=	area under the curve
CI	=	confidence interval
FDG	=	F-18 fluorodeoxyglucose
LAD	=	left anterior descending artery
LCX	=	left circumflex artery
LV	=	left ventricle or left ventricular
MI	=	myocardial infarction
PET	=	positron emission computed tomography
PTCA	=	percutaneous transluminal coronary angioplasty
RCA	=	right coronary artery
ROC	=	receiver operator curve
RWM	=	regional wall motion
SPECT	=	single photon emission computed tomography

to eliminate discrepancies induced by spontaneous changes of global or regional function between the diagnostic catheterization and the time of endocardial mapping. The coronary intervention was performed immediately after obtaining the electroanatomic map.

The institutional ethical committee approved the study protocol, and patients gave informed consent.

Electroanatomic mapping and data postprocessing. The intraventricular mapping and navigation system (NOGA, Biosense-Webster, Diamond Bar, California) has been described in detail previously (2,5).

Unipolar signals filtered at 0.5 Hz to 400 Hz were recorded in this study, and an interpolation threshold of 40 mm was used. Maps of unipolar electrogram amplitudes were obtained by displaying the peak-to-peak amplitude of the unipolar electrogram on a graded color scale.

Additionally, mechanical maps were reconstructed using the function of linear local shortening. In principle, this parameter is calculated for each point as the mean value of the systolic linear movement of every surrounding acquired point in the direction of the point (normalized to the distance during diastole) (5).

In this study, the position of the reconstructed apex was compared to the apex of the biplane LV angiogram obtained before mapping and reset manually in case of discordant findings.

Points were deleted from the map if one of the following criteria was met:

1) Loop stability (mean distance between the location of the catheter at two consecutive beats at corresponding time points in the cardiac cycle) was >6 mm;
2) Location stability (distance of the end-diastolic catheter tip location between two consecutive heart beats) was >6 mm;
3) Deviation from the mean cycle length was >15%;
4) One of two consecutive beats was a premature beat;
5) Two consecutive endocardial electrograms were different in morphology; or
6) Two consecutive QRS complexes of the surface electrocardiogram were different in morphology.

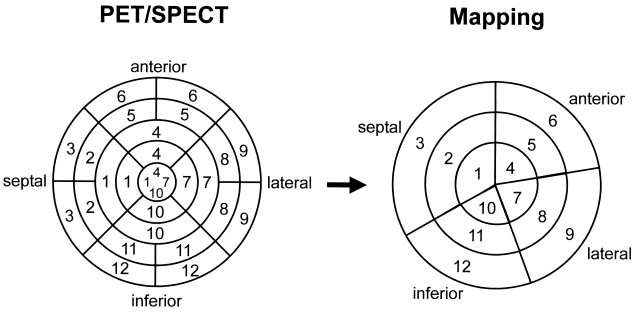

Figure 1. Polar plot and segmentation of the LV for positron emission computed tomography (PET)/single photon emission computed tomography (SPECT) and mapping analysis. The segmentation methods for both modalities are described in detail in the Methods section. Positron emission computed tomography/SPECT regions (n = 25) were grouped (see numbers), and mean values were calculated and assigned (same numbers for corresponding regions) to the mapping regions (n = 12).

Additionally, inner points were deleted from the map using a computer algorithm. It compares the relative depth of a point within the reconstruction with its neighboring points localized within a cone formed around a line connecting the investigated point and the center of the reconstruction (tip of the cone). Points with a relative depth >10% using a cone angle of 25° were deleted from the map.

A polar projection of the LV along an axis from the center of mass of the reconstructed ventricle to the apex was generated. The reconstructed ventricle was divided into three parts (apex, midventricle and base, consisting of 20%, 40% and 40% of the long-axis length, respectively), and the longitudinal location of each endocardial site was determined on the basis of its projection on this axis. The three parts were each further divided into four regions: septal (120° of the circumference), anterior (80°), lateral (80°) and inferior (80°) (Fig. 1). Thus, in this polar view, the ventricle was divided into 12 regions. Mean values for the peak-to-peak amplitudes of the unipolar electrograms were calculated for each region.

Technetium-99m sestamibi SPECT imaging. Since an on-site cyclotron is not available at our institution, we use a combination of perfusion imaging with Tc99m sestamibi SPECT and metabolic imaging with F-18 fluorodeoxyglucose (FDG) for myocardial viability assessment (11,12). Nuclear studies were performed after diagnostic catheterization and before the mapping and PTCA. Patients were studied at rest 2 h after injection of 10 mCi Tc-99m sestamibi with a light meal after tracer application. Data were acquired using a double head gamma camera (Solus, ADAC Lab., Milpitas, California), axial full field of view 55.5 cm and matrix size 128 × 128. Reconstruction including attenuation and scatter correction was performed as described before (13).

Fluorine-18 FDG PET imaging. After transmission imaging and glucose loading with 50 g dextrose orally, 6 to 8 mCi FDG were injected. Static imaging for 30 to 40 min was initiated 30 to 45 min after tracer injection using a PET scanner ECAT EXACT (CTI, Knoxville, Tennessee),

Table 1. Unipolar Electrogram Amplitude and Linear Local Shortening in Regions Defined by Nuclear Imaging

PET/SPECT Imaging (definitions)	n	Unipolar Electrogram Amplitude (mV)	Local Shortening (%)	Unipolar Electrogram Amplitude (mV)/Patients With All Types of Regions (n = 27)	Local Shortening (%)/ Patients With All Types of Regions (n = 27)
Normal Perfusion (sestamibi uptake > 70%)	46	11.8 ± 3.6 (9.1–14.6)	8.9 ± 4.1 (4.7–13.4)	11.0 ± 3.6* (8.2–12.8)	7.3 ± 3.8*† (4.1–10.3)
Reduced perfusion, preserved metabolism (sestamibi uptake < 70% & FDG uptake ≥50%)	45	9.4 ± 3.0 (6.7–11.4)	5.7 ± 4.0 (2.1–8.5)	9.0 ± 2.8* (6.8–11.1)	4.6 ± 3.5† (2.3–7.1)
Scar (sestamibi uptake & FDG uptake <50%)	28	6.5 ± 2.5 (4.6–7.2)	1.7 ± 4.7 (−0.6–6.7)	6.5 ± 2.6* (4.6–7.6)	1.5 ± 4.7*† (−0.7–5.0)

*$p < 0.001$; †$p < 0.01$. Numbers in brackets represent 25% to 75% percentiles.
FDG = F-18 fluorodeoxyglucose; PET = positron emission computed tomography; SPECT = single photon emission computed tomography.

matrix size 128 × 128, axial field of view 49.7 cm and axial width 15 cm in three bed positions. Reconstruction was performed by filtered back projection (Hanning, cutoff frequency 0.4 and zoom 1.12). Positron emission tomography and SPECT imaging were performed on the same day in all patients.

PET and SPECT analysis. Left ventricular long axis was defined interactively, and quantitative analysis was performed in the two data sets using a vector based automatic segmentation program (modified ECAT software, CTI) (14). The values of 450 vector profiles for SPECT and PET studies were assigned to 33 regions of a polar map. Sestamibi and FDG uptake was expressed as percentage of the region with the maximal sestamibi uptake. The polar map divides the ventricle into six slices, each covering approximately 17% of the long-axis length. Because high variations are usually found in the most basal regions, the outer slice was not considered for analysis. As shown in Figure 1, the four remaining outer slices were further subdivided into anterior, septal, inferior and lateral regions (each 90° of the circumference); the apical slice was not further subdivided.

In order to compare nuclear and mapping data on a regional basis, 25 regions of the PET and SPECT datasets were assigned to the 12 regions of the electroanatomic regional polar map. Since both modalities use different segmentation methods, nuclear regions had to be arranged as shown in Figure 1, and the mean uptake value was calculated.

The applied definitions for myocardial viability based on the literature (11,15–18) are shown in Table 1.

Analysis of RWM. Regional wall motion was analyzed using a modified centerline method (QUANTCOR.LVA, Siemens, Germany) from digitized angiograms (19). Vessel territories were assigned to contiguous chords as previously described (19). Regional wall motion was assessed in the territory of the target vessel and in the territory of a patent and noninfarct-related vessel in each patient. Left ventricular ejection fraction was determined by the area-length method from the 30° right anterior oblique angiogram.

Statistical analysis. Data are presented as mean ± SD. Data were analyzed on a patient basis. In a first approach, all regions were included in the analysis, and values were averaged for a given region type for a given patient, thereby obtaining a single value for that region type for that patient. In a second approach, the value of the region representing the center of the infarct area was used in every patient. Differences in continuous variables were measured using repeated measures analysis of variance with Bonferroni post hoc analysis and Student *t* test for paired and unpaired samples. Receiver operating curve (ROC) analysis was performed with MedCalc 4.16a software (Mariakerke, Belgium). Spearman correlation coefficients were calculated.

RESULTS

Patients. Forty-six patients (32 men, 59 ± 10 years) were included in the study. Twenty-six patients had an anterior MI; 14 patients had an inferior MI. Six patients had no clinical history of MI but had severe RWM abnormalities in the territory of the target vessel (two inferior, four anterior). The median time interval from infarction to revascularization was 88 days and from PET/SPECT imaging to mapping and revascularization was 24 days. Clinically, there was no evidence for cardiac events between PET/SPECT imaging and mapping. Angiographic ejection fraction was 49 ± 15%. Twenty-four patients had single-vessel disease; 16 patients had two-vessel disease; and 6 patients had three-vessel disease. Target lesions were located in the LAD in 27 patients, in the RCA in 12 patients, in the LCX in 4 patients and in bypass grafts in 3 patients (one LAD, two RCA). Twenty-two patients had a complete occlusion of the target vessel.

PET/SPECT imaging and electroanatomic mapping. The nuclear polar maps of the 46 patients were divided into 12 regions matching the mapping polar maps. Due to technical difficulties, no mapping points were acquired in 17 regions, and these regions were subsequently not considered for quantitative analysis. Results of PET/SPECT analysis are shown in Table 1.

The average number of points acquired per patient after postprocessing was 76 ± 18, with 6 ± 2 points per region. The time to obtain a complete map was 52 ± 21 min. The minimal recorded value for the regional unipolar amplitude was 1.3 mV, and the highest value was 29.8 mV, with a mean value of 10.4 mV ± 4.7 mV. No complications occurred during the mapping procedures.

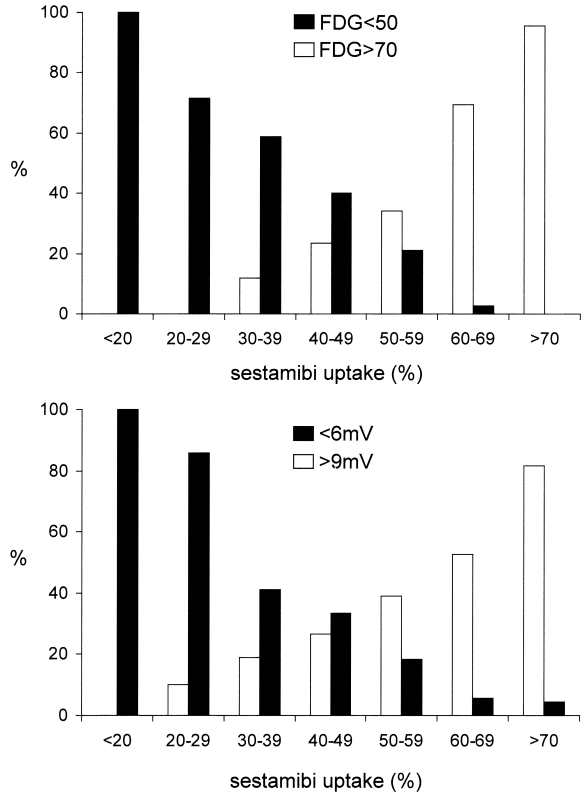

Figure 2. Percentage of regions with normal and absent metabolism **(upper panel)** and electrical activity **(lower panel)**, respectively, in relation to sestamibi uptake. In the **upper panel**, normal metabolism is defined by an F-18 fluorodeoxyglucose (FDG) uptake ≥70% and absent metabolism by an uptake <50%. In the **lower panel**, normal electrical activity is defined by an electrogram amplitude >9 mV and absent activity as <6 mV.

Comparison of electroanatomic mapping and PET/SPECT results. The regional unipolar amplitude was significantly different between normally perfused regions, regions with reduced perfusion but preserved metabolism and scar regions (Table 1).

The percentage of regions with an FDG uptake >70% ranged from 12% in regions with severe Tc-99m defects and up to 34% in regions with moderate Tc-99m defects (Fig. 2). Similar results were found for the unipolar electrogram amplitude; the percentage of regions with an amplitude >9 mV ranged from 19% in regions with severe Tc-99m defects up to 39% in regions with moderate Tc-99m defects (Fig. 2). In regions with severely reduced sestamibi uptake (<50%) but preserved FDG uptake (≥50%), the unipolar electrogram amplitude was 8.1 mV ± 3.6 mV, compared with 6.6 mV ± 2.7 mV in regions with severely reduced sestamibi uptake and concordantly reduced FGD uptake (both <50%).

To assess the ability of electroanatomic mapping of regional unipolar amplitudes for discrimination of viable and scar regions, a ROC analysis comparing regions with evidence of maintained viability (normal regions and regions with reduced perfusion but preserved metabolism) with scar regions was performed on a patient basis (original regions n = 536). The area under the curve (AUC) was 0.84 (95% confidence interval (CI): 0.76 to 0.90) (Fig. 3). After exclusion of the most basal regions with mean regional amplitudes <6 mV, the analysis of the remaining regions (n = 500) yielded an AUC of 0.88 (95% CI: 0.81 to 0.93). Using a threshold electrogram amplitude of 7.5 mV, the sensitivity and specificity for detecting viable myocardium were 77% and 75%, respectively. At 6 mV the sensitivity was 96% (specificity 57%), and at 9 mV the specificity was 82% (sensitivity 65%). After exclusion of the most basal regions with mean regional amplitudes <6 mV, sensitivity and specificity (threshold 7.5 mV) were 85% and 81%, respectively.

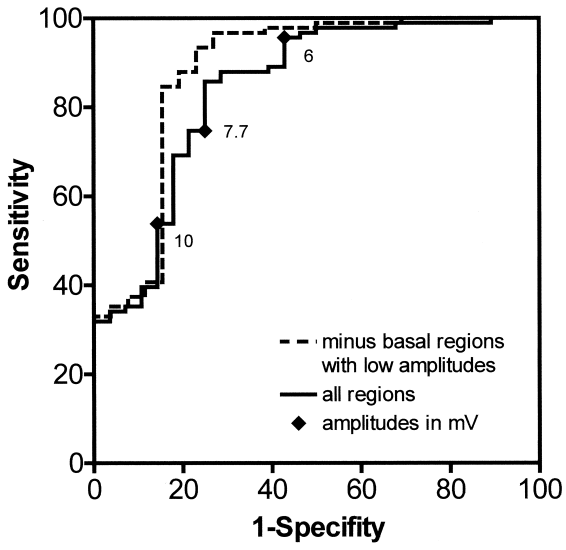

Figure 3. Receiver operator curve (ROC) analysis for detection of viable regions (normal perfusion, reduced perfusion but preserved metabolism) versus scar regions by the unipolar electrogram amplitude on a patient basis. The **solid line** represents the ROC curve for all regions (original regions n = 536); the **dashed line** represents the ROC curve for all regions minus the basal regions with regional unipolar amplitudes <6 mV (n = 500).

For the septal regions (regions 1 to 3 in Fig. 1), the ROC analysis revealed an AUC of 0.83, for the anterior regions (regions 4 to 6), 0.76; for the lateral regions (regions 7 to 9), 0.94 and for the inferior regions (regions 9 to 12), 0.90.

Images of a patient with an apical scar and reduced perfusion but preserved FDG uptake in the surrounding anterior myocardium are illustrated in Figure 4. The corresponding unipolar amplitude map displays an area of low amplitude only in the apical region, whereas the rest of the anterior wall had higher unipolar amplitudes indicating preserved viability.

Linear local shortening was significantly different among normally perfused myocardium, regions with reduced perfusion and scar regions (Table 1). The ROC analysis for identification of scar revealed an AUC of 0.81 (95% CI: 0.73 to 0.88). Combining the information from linear local shortening and the unipolar electrogram amplitude (AUC of 0.86 [95% CI: 0.79 to 0.92]) did not increase the diagnostic accuracy compared with the analysis of the unipolar electrogram amplitude alone. Linear local shorten-

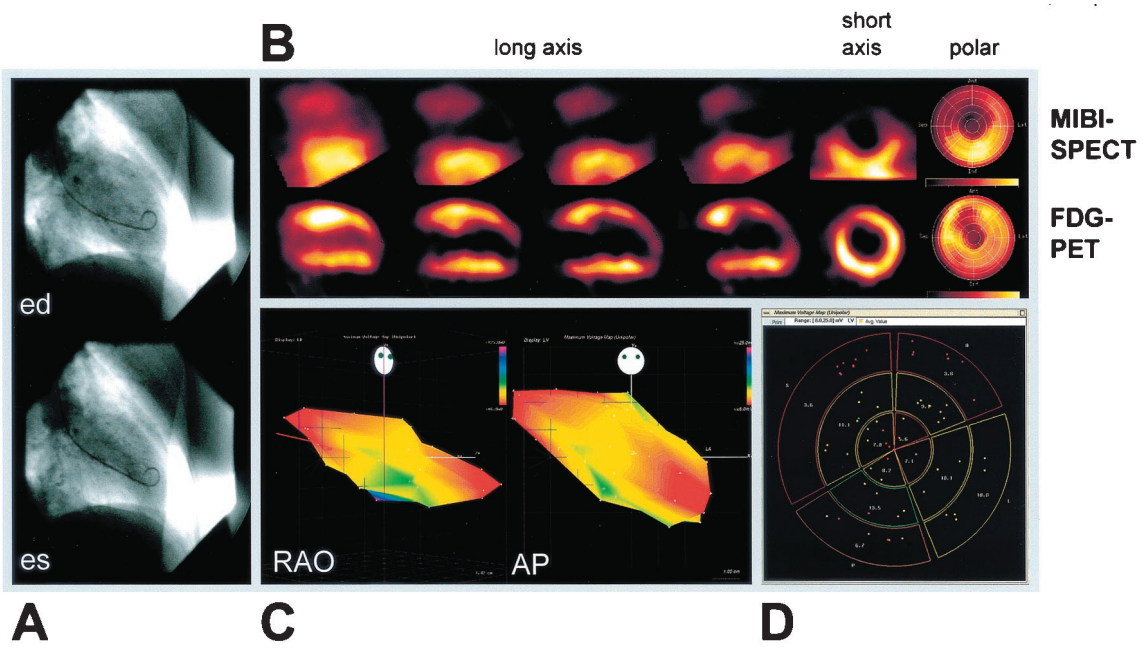

Figure 4. **(A)** Right anterior oblique view of the left ventricular angiogram at end-diastole (ed) and end-systole (es) of a patient with severe hypokinesia of the anterior wall after anterior myocardial infarction. **(B)** Long- and short-axis positron emission computed tomography (PET) and single photon emission computed tomography (SPECT) images and corresponding polar maps showing an apical scar and reduced perfusion but preserved F-18 fluorodeoxyglucose (FDG) uptake in the surrounding anterior wall. **(C)** Unipolar amplitude map of the LV obtained by endocardial mapping (**left:** right anterior oblique view [RAO]; **right:** anteroposterior [AP] view). Color coding ranges from <6 mV **(red)** to >25 mV **(purple)**. The apex is displayed with low amplitude, whereas the adjacent anterior wall has higher amplitudes. **(D)** Regional polar view of the unipolar amplitude map of the LV, divided into 12 regions. MIBI = Tc 99m sestamibi.

ing correlated with the regional unipolar electrogram amplitude ($r = 0.57$, $p < 0.001$).

Comparison of electroanatomic mapping with PET/SPECT and RWM in infarct area. For comparison of electroanatomic mapping with PET/SPECT and RWM, we performed an analysis per infarct area using the value of the region representing the center of the infarct area.

In patients with nonviable myocardium by nuclear imaging, the unipolar electrogram amplitude was 6.1 mV ± 2.0 mV in the infarct area, whereas, in patients with viable myocardium, the unipolar electrogram amplitude was 11.4 mV ± 3.6 mV in the infarct area ($p < 0.001$). The AUC by ROC analysis was 0.92 (95% CI: 0.80 to 0.98). At a threshold amplitude of 7.5 mV, the sensitivity was 90% and the specificity was 81%. The corresponding values for local shortening were 2.0 ± 4.5% for nonviable and 7.2 ± 5.4% ($p < 0.01$) for viable myocardium with an AUC of 0.77 (95% CI: 0.63 to 0.88).

Linear local shortening, as a parameter of regional mechanical function derived from electromechanical mapping, was 4.3 ± 5.5% in infarct areas versus 11.0 ± 4.8% in remote control areas ($p < 0.001$). Regional unipolar amplitude in these areas was 8.4 mV ± 3.9 mV and 13.3 mV ± 4.0 mV ($p < 0.001$), respectively. Linear local shortening correlated with the regional unipolar electrogram amplitude ($r = 0.56$, $p < 0.001$).

Unipolar electrogram amplitude and linear local shortening did not differ between anterior infarcts and inferior infarcts (7.6 mV ± 2.8 mV vs. 8.6 mV ± 4.8 mV, $p = NS$ and 3.2 ± 4.7% vs. 5.5 ± 5.4%, $p = NS$, respectively).

There was a significant correlation between linear local shortening and RWM with $r = 0.61$ ($p < 0.001$) but no correlation between regional electrogram amplitude and RWM ($r = -0.13$, $p = NS$).

Results of electroanatomic mapping and PET/SPECT imaging versus recovery of global and regional LV function. Follow-up angiography was performed after six months in 28 patients demonstrating patent revascularized vessels with a diameter stenosis <50% in 25 patients. Seven patients did not undergo follow-up angiography, because of either unsuccessful recanalization (two patients), death (two patients), reinfarction (two patients) or ischemic disabling stroke (one patient) during follow-up. Eleven patients were lost to follow-up (three patients) or did not consent to follow-up angiography (eight patients).

Left ventricular ejection fraction improved significantly from 52 ± 16% to 62 ± 13% ($p = 0.01$) in 13 patients in which mapping of infarct areas had shown regional unipolar electrogram amplitudes >7.5 mV, whereas ejection fraction did not change (50 ± 12% to 50 ± 11%) in 12 patients with regional unipolar amplitudes <7.5 mV in the target area.

Similarly, RWM improved from −2.4 SD/chord ± 1.0 SD/chord to −1.5 SD/chord ± 1.1 SD/chord ($p < 0.01$) in infarct areas with electrogram amplitudes >7.5 mV, whereas RWM remained unchanged (−2.3 SD/chord ±

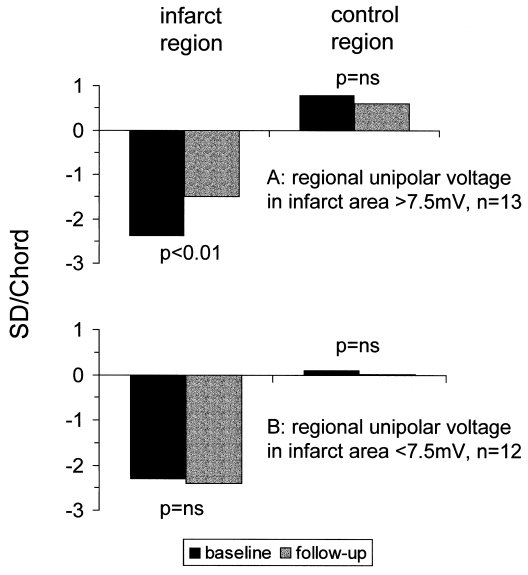

Figure 5. Regional wall motion in the infarct area and control area before and six months after successful percutaneous transluminal coronary angioplasty in patients with regional unipolar electrogram amplitudes in the infarct area >7.5 mV (n = 13) and in patients with regional unipolar electrogram amplitudes in the infarct area <7.5 mV (n = 12). SD = standard deviation.

0.7 SD/chord before revascularization vs. −2.4 SD/chord ± 0.7 SD/chord at follow-up, p = NS) in infarct areas with amplitudes <7.5 mV. Regional wall motion in control areas did not change significantly (0.8 ± 1.5 SD/chord to 0.6 ± 1.7 and 0.1 ± 1.4 to 0.0 ± 1.0 SD/chord, respectively) (Fig. 5).

The unipolar electrogram amplitude was significantly higher in functionally recovering areas than it was in areas without improvement after revascularization (10.2 mV ± 2.4 mV vs. 6.6 mV ± 2.2 mV, p < 0.01). Endocardial mapping at a threshold of 7.5 mV had a sensitivity of 91% and a specificity of 71%, whereas PET/SPECT imaging had a sensitivity of 82% and a specificity of 86% for recovery of RWM (+0.5 SD/chord).

DISCUSSION

Assessment of myocardial viability. The purpose of this study was to compare the assessment of myocardial viability by endocardial catheter-based electroanatomic mapping with metabolic imaging using FDG-PET and, furthermore, with data on functional recovery after successful revascularization. The results indicate that myocardial regions identified as scar regions by PET/SPECT imaging have significantly lower mean regional unipolar amplitudes than regions identified as viable. Moreover, unipolar electrogram amplitudes correlated with recovery of regional and global ventricular function after successful revascularization.

Unipolar electrogram amplitudes were significantly different among normal regions, regions with reduced perfusion but preserved metabolism and scar regions (Table 1). The ROC analysis revealed an AUC of 0.84, a value that is commonly considered as sufficient for a diagnostic procedure (Fig. 3). Sensitivity and specificity were in the range reported for other diagnostic modalities of viability assessment.

As described previously (11), FDG-PET could demonstrate preserved metabolism in some of those regions with moderate-to-severe perfusion defects. Similarly, electroanatomic mapping identified a considerable number of regions with perfusion defects as "electrically viable" (Fig. 2). Preserved unipolar electrogram amplitudes, despite severely reduced myocardial perfusion, have also been demonstrated in a pig model using contrast echocardiography and electromechanical mapping five weeks after placement of an ameroid constrictor around the circumflex artery (8).

Regional electrical function correlated closely with recovery of RWM after successful revascularization (Fig. 5). Furthermore, electrogram amplitudes were significantly higher in recovered regions than they were in regions without functional improvement.

These data suggest strongly that the electrogram amplitude can be used as a marker of myocardial viability. The presented data confirm and extend, by serial functional assessment, the findings of Kornowski et al. (20) who used thallium-201 SPECT as the reference method for viability assessment.

Linear local shortening as a mapping parameter of mechanical function correlated with angiographically assessed RWM. Although linear local shortening was significantly smaller in scar regions than in regions with reduced perfusion but preserved metabolism, the discrimination was less efficient by ROC analysis, and a combination of both parameters did not increase the accuracy for discrimination between viable and nonviable myocardium.

Study limitations. In this study, electromechanical maps were compared with PET/SPECT and RWM data. The segmentation of the LV is not identical for the three methods. Misalignment of the corresponding regions may lead to discordant findings and a certain degree of error. It is possible that the results, in fact, underestimate the diagnostic accuracy of electroanatomic mapping.

Positron emission tomography/SPECT imaging were not performed at the same time as endocardial mapping. This may be a source of error, but we consider perfusion and metabolism in these patients with chronic MI stable enough to make changes over three to four weeks unlikely. Additionally, since PET/SPECT imaging was always performed before mapping, the error should be systematic and similar for all patients.

Analysis of other electrophysiologic parameters that could be obtained during endocardial mapping may improve the diagnostic performance of the mapping system for viability assessment. These include fractionation of electrograms (21), amplitude to duration ratio and electromechanical delay. Novel signal processing methods may be able to discriminate better between nonviable and viable myocardium (22).

Electromechanical mapping of the basal parts of the LV includes sites on the valve apparatus with low endocardial amplitudes due to its fibrous nature. Inclusion of these points lowers the mean regional amplitude and may produce false negative results for the regional myocardial viability of the most basal parts of the LV. In the presented analysis, the diagnostic accuracy improved after exclusion of the most basal regions, with regional amplitudes below 6 mV.

It should be emphasized that the accuracy of the method for assessing viability is likely to be influenced by the point density and by the training of the interventional cardiologist. With regard to point density, sampling more points per entire map and more points per region might further increase the accuracy of the method. However, this would be associated with a prolonged mapping time. Mapping of one region representing the infarct area also allowed an accurate discrimination of viable and nonviable myocardium, as our analysis showed. With regard to training, we believe that a training period in 5 to 10 patients is sufficient for an experienced interventional cardiologist or electrophysiologist to perform mapping procedures of good diagnostic quality.

Finally, these data represent the early experience with the mapping system and are derived from a relatively small number of patients. Certainly, studies in larger patient populations are needed to confirm our findings.

Clinical implications. Endocardial electroanatomic mapping can be used in patients with prior MI and RWM abnormalities to assess myocardial viability in the catheterization laboratory in combination with diagnostic coronary angiography. It should provide immediate information about the viability status of the infarcted myocardium and guide the interventional cardiologist in the decision to perform an ad hoc revascularization or surgical intervention without further viability assessment.

Given the existing financial restraints within most health care systems, the cost of the different methods for myocardial viability assessment must be considered. Currently, the costs for an FDG PET/Tc99m sestamibi SPECT at our institution are $1,100 and, for a thallium-201 SPECT, $300.00. The costs for a mapping procedure (reference and mapping catheter) are currently $2,300. This difference may be counterbalanced by the advantage of an ad hoc PTCA guided by an on-line viability assessment by mapping. However, for making a viability assessment by endocardial mapping a more attractive alternative to conventional nuclear imaging, a reduction in costs would be appropriate.

Endocardial electroanatomic mapping may also be used in the setting of catheter-based direct myocardial revascularization (23). Scar areas and viable myocardium can be identified and visualized with this technique, and subsequent revascularization procedures can be targeted to viable regions, avoiding unnecessary treatment of scar tissue.

Reprint requests and correspondence: Dr. Jürgen vom Dahl, Medizinische Klinik I, Universitätsklinikum der RWTH Aachen, Pauwelstrasse 30, D-52057 Aachen, Germany. E-mail: jvomdahl@post.klinikum.rwth-aachen.de.

REFERENCES

1. Ben-Haim SA, Osadchy D, Schuster I, Gepstein L, Hayam G, Josephson ME. Nonfluoroscopic, in vivo navigation and mapping technology. Nat Med 1996;2:1393–5.
2. Gepstein L, Hayam G, Ben-Haim SA. A novel method for nonfluoroscopic catheter-based electroanatomical mapping of the heart: in vitro and in vivo accuracy results. Circulation 1998;95:1611–22.
3. Downar E, Janse MJ, Durrer D. The effect of acute coronary artery occlusion on subepicardial transmembrane potentials in the intact porcine heart. Circulation 1977;56:217–24.
4. Franz MR, Flaherty JT, Platia EV, Bulkley BH, Weisfeldt ML. Localization of regional myocardial ischemia by recording of monophasic action potentials. Circulation 1984;69:593–604.
5. Gepstein L, Goldin A, Lessick J, et al. Electromechanical characterization of chronic myocardial infarction in the canine coronary occlusion model. Circulation 1998;98:2055–64.
6. Kornowski R, Hong MK, Gepstein L, et al. Preliminary animal and clinical experiences using an electromechanical endocardial mapping procedure to distinguish infarcted from healthy myocardium. Circulation 1998;98:1116–24.
7. Fuchs S, Kornowski R, Shiran A, Pierre A, Ellaham S, Leon M. Electromechanical characterization of myocardial hibernation in a pig model. Coron Artery Dis 1999;10:195–8.
8. Van Langenhove G, Hamburger JN, Smits PC, et al. Evaluation of left ventricular volumes and ejection fraction with a nonfluoroscopic endoventricular three-dimensional mapping technique. Am Heart J 2000;140:596–602.
9. Van Langenhove G, Hamburger JN, Roelandt JRTC, et al. Comparison of mechanical properties of the left ventricle in patients with severe coronary artery disease by nonfluoroscopic mapping versus two-dimensional echocardiograms. Am J Cardiol 2000;86:1047–50.
10. Lessick J, Smeets JL, Reisner SA, Ben-Haim SA. Electromechanical mapping of regional left ventricular function in humans: comparison with echocardiography. Cath Cardiovasc Interv 2000;50:10–8.
11. Altehoefer C, vom Dahl J, Biedermann M, et al. Significance of defect severity in technetium-99m-MIBI SPECT at rest to assess myocardial viability: comparison with fluorine-18-FDG PET. J Nucl Med 1994; 35:569–74.
12. vom Dahl J, Altehoefer C, Sheehan FH, et al. Recovery of regional left ventricular dysfunction after coronary revascularization: impact of myocardial viability assessed by nuclear imaging and vessel patency at follow-up angiography. J Am Coll Cardiol 1996;28:948–58.
13. Kupferschläger J, Müller B, Schulz G, et al. A method for combined scatter and attenuation correction without transmission measurement for myocardial SPECT with 99m-Tc binding. Nuklearmedizin 1997; 36:56–64.
14. Laubenbacher C, Rothley J, Sitomer J, et al. An automated analysis program for the evaluation of cardiac PET studies: initial results in the detection and localization of coronary artery disease using nitrogen-13-ammonia. J Nucl Med 1993;34:969–78.
15. Dilsizian V, Arrighi JA, Diodati JG, et al. Myocardial viability in patients with chronic coronary artery disease: comparison of 99mTc-sestamibi with thallium reinjection and (18F)fluorodeoxyglucose. Circulation 1994;89:578–87.
16. Maes AF, Borgers M, Flameng W, et al. Assessment of myocardial viability in chronic coronary artery disease using technetium-99m sestamibi SPECT. J Am Coll Cardiol 1997;29:62–8.
17. Baer FM, Voth E, Deutsch HJ, et al. Predictive value of low-dose dobutamine transesophageal echocardiography and fluorine-18 fluorodeoxyglucose positron emission tomography for recovery of regional left ventricular function after successful revascularization. J Am Coll Cardiol 1996;28:60–9.
18. Srinivasan G, Kitsiou AN, Bacharach SL, Bartlett ML, Miller-Davis C, Dilsizian V. (18F)Fluorodeoxyglucose single photon emission computed tomography. Can it replace PET and thallium

SPECT for the assessment of myocardial viability? Circulation 1998;97:843–50.
19. Sheehan FH, Bolson EL, Dodge MD, Mathey DG, Schofer J, Woo H-K. Advantages and applications of the centerline method for characterizing regional ventricular function. Circulation 1986;74:293–305.
20. Kornowski R, Hong MK, Leon MB. Comparison between left ventricular electromechanical mapping and radionuclide perfusion imaging for detection of myocardial viability. Circulation 1998;98:1837–41.
21. Gardner PI, Ursell, PC, Fenoglio JJ, Wit AL. Electrophysiologic and anatomic basis for fractionated electrograms recorded from healed myocardial infarcts. Circulation 1985;72:596–611.
22. Ellis WS, Eisenberg SJ, Auslander DM, Dae MW, Zakhor A, Lesh MD. Deconvolution: a novel signal processing approach for determining activation time from fractionated electrograms and detecting infarcted tissue. Circulation 1996;94:2633–40.
23. Kornowski R, Bhargava B, Leon M. Percutaneous transmyocardial laser revascularization: an overview. Cath Cardiovasc Interv 1999;47: 354–9.